

## Real-time x-ray-scattering measurement of the nucleation kinetics of cubic gallium nitride on $\beta$ -SiC(001)

R. L. Headrick, S. Kycia, and Y. K. Park\*

*Cornell High Energy Synchrotron Source, Cornell University, Ithaca, New York 14853*

A. R. Woll and J. D. Brock

*School of Applied and Engineering Physics, Cornell University, Ithaca, New York 14853*

(Received 3 April 1996)

We have performed a real-time x-ray-scattering study of the nucleation of cubic GaN on SiC(001) during metal-organic molecular-beam epitaxy. By monitoring both the Ga fluorescence and the diffracted intensity from the GaN film, we determine the growth rate and crystalline quality from submonolayer coverage to 350 nm. The results exhibit scaling behavior in the growth kinetics consistent with quasi-two-dimensional island growth. In this growth mode, three-dimensional nuclei form and then grow laterally until coalescence into a continuous film occurs. After coalescence, the growth rate drops to its steady-state value.

[S0163-1829(96)05944-9]

### I. INTRODUCTION

Development of new epitaxial growth techniques requires a detailed understanding of the fundamental physical processes of thin-film growth, such as nucleation, aggregation, and coalescence of islands on a planar substrate.<sup>1,2</sup> Most studies of nucleation during epitaxial growth have been concerned with molecular-beam epitaxy (MBE). In contrast, relatively little experimental work has focused on surface processes in the early stages of gas-source (GS) molecular-beam epitaxy. The two cases are usually distinguished by the adatom (or admolecule) lifetime on the surface  $\tau$  compared to the time to deposit a monolayer of material. In the more familiar case of deposition from an evaporation source when  $\tau$  is long, the sticking coefficient is close to one and the growth rate may be taken to be simply proportional to the flux. If the lifetime is short, then adparticles have a high probability of escaping before diffusing to an active site and being incorporated into the surface. Site-specific chemical reactions and multiple surface species further complicates the GS-MBE growth process. In general, gas-source growth is a complicated function of temperature, molecular impingement rates, surface morphology, and surface composition.

The main result of this paper is that the growth rate varies with the size distribution of overcritical nuclei. The size distribution of islands during growth of two-dimensional nuclei exhibits scaling behavior, as recently discussed by Family and Amar.<sup>3</sup> This scaling behavior is directly observable using real-time x-ray measurement of the coverage in GS-MBE. While Ref. 3 discusses only two-dimensional island growth, we observe similar scaling behavior for three-dimensional island growth. Our results are for the case of the cubic or  $\beta$  phase of GaN grown onto a cubic SiC(001) substrate. However, the growth model presented is applicable to many other systems.

#### A. Growth by nucleation and coalescence

The theory of thin-film nucleation rates and cluster growth is well developed.<sup>4,5</sup> A large number of experimental

studies have been performed that support its basic assumptions.<sup>6,7</sup> Qualitatively, the theory is as follows: Initially, nuclei form from a supersaturation of adatoms on the surface. Subcritical nuclei dissolve again, but nuclei that reach a critical size begin to grow. Although this basic theory is well established, very few nucleation experiments have been performed on systems that exhibit surface lifetime limited growth kinetics.<sup>8</sup>

There are two possible routes for adsorbed atoms or molecules to be incorporated into growing islands. The first is direct impingement onto the growing island. The second is by adsorption onto the substrate followed by surface diffusion and capture by a growing island. There are two corresponding categories of island growth morphology. (i) If the islands are hemispherical, or cap shaped, then the growth rate is proportional to the projected surface area. Growth of large cap-shaped islands is dominated by the direct impingement of vapor, although surface capture may also contribute to the growth. (ii) If the islands are disk shaped, i.e., they grow rapidly in two dimensions, then the growth rate varies as their diameter. We will call this type of growth quasi-two-dimensional since the thickness of nuclei may reach 100 ML or more, but increases slowly compared to the lateral dimensions. Disk-shaped nuclei grow predominantly by diffusion from the free substrate to the edge of the nuclei and by surface diffusion from the center. Both cap-shaped and disk-shaped island growth lead to power-law behavior. After the nuclei coalesce into a continuous film, the growth reaches its steady-state rate.

In our experiment we use metal-organic molecular-beam epitaxy to grow GaN on SiC(001). The precursors are ammonia and triethyl-gallium. Ammonia has a very low efficiency for nucleating and growing GaN.<sup>9-12</sup> This leads to a low density of nearly noninteracting nuclei in the early stages of deposition. Therefore, direct measurement of island growth kinetics may be obtained by a simple measurement of the deposition rate. Below, we give experimental details and then describe GaN growth on SiC.

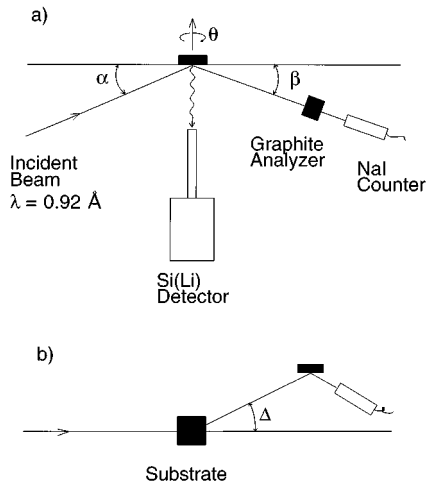


FIG. 1. Diagram of the experimental arrangement. The sample is mounted inside an ultrahigh vacuum enclosure with gas injectors and a heater for the film growth (not shown). The incident beam, scattered x rays, and x-ray fluorescence pass into and out of the chamber through beryllium windows. The apparatus allows independent adjustment of the angles  $\alpha$ ,  $\beta$ ,  $\theta$ , and  $\Delta$ .

## II. EXPERIMENT

### A. Apparatus

The experiment was done at the A2 experimental station at the Cornell High Energy Synchrotron Source using radiation from a 1.2-T, 24-pole permanent magnet wiggler. X rays were directed onto a two crystal Si(111) monochromator with a sagittally bent second crystal for focusing. The flux at the experiment was  $\approx 10^{12}$  photons per second in a 0.5-mm-vertical by 3-mm-horizontal beam spot at a wavelength of 0.092 nm. X rays illuminated a sample inside a turbomolecular pumped ultrahigh vacuum surface diffraction chamber with a base pressure of  $1 \times 10^{-10}$  Torr. A manipulator stage in the chamber allows samples to be mounted on it with a horizontal surface normal. The manipulator has two orthogonal high-resolution rotation axes and a built-in heater capable of heating the sample to 1000 °C. A detector arm with rotation stages for a crystal analyzer and a NaI(Tl) detector is mounted in a vertical scattering geometry. The entire experiment including the chamber and detector assembly rests on a table that can rotate in the horizontal plane. The combined rotations allow for the angles  $\alpha$ ,  $\beta$ ,  $\theta$ , and  $\Delta$ , as defined in Fig. 1, to be varied independently by computer control using the SPEC software package.<sup>13</sup> A graphite crystal analyzer with a mosaic width of  $0.4^\circ$  was used to filter out fluorescence background from the diffracted beam. Out-of-plane resolution and active area were defined by  $2 \times 2$  mm<sup>2</sup> slits in front of the NaI(Tl) detector. A Si(Li) detector was mounted along the surface normal to monitor Ga  $K\alpha$  fluorescence.

### B. Surface preparation and film growth

A substrate consisting of a 5- $\mu$ m film of  $\beta$ -SiC(001) grown on an on-axis Si(001) wafer was chemically oxidized in a 3:1:1 solution of HCl:H<sub>2</sub>O<sub>2</sub>:H<sub>2</sub>O before it was introduced into the chamber. The SiC surface was cleaned in vacuum by heating to 950 °C for 5 min. The temperature was reduced to 600 °C for growth. GaN was deposited by

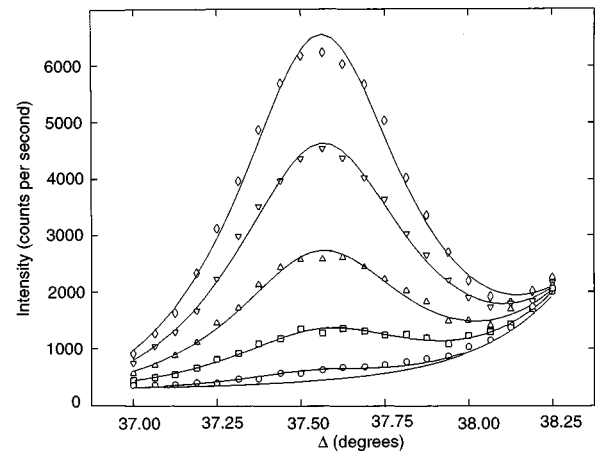


FIG. 2. Scans of the detector angle  $\Delta$  at six different times during the GaN film growth. The base-line curve without any data points is a fit to the curve taken just before opening the gas valves. The other curves have the following symbols for the data and times (in seconds): circles, 500; squares, 1000; upward pointing triangles, 1500; downward pointing triangles, 2000; diamonds, 2500. The  $\alpha$  and  $\beta$  angles were fixed at  $5.84^\circ$ .

introducing triethylgallium and ammonia through gas injectors. Molecular impingement rates for triethylgallium and ammonia were  $9.6 \times 10^{14}$  and  $4.2 \times 10^{18}$  cm<sup>-2</sup> s<sup>-1</sup>, respectively. The background pressure in the chamber under these conditions was  $2 \times 10^{-3}$  Torr. The GaN film grows to a thickness of 350 nm during a 90-min interval.

### C. Data collection

Film coverage and structure were monitored simultaneously in real time during the entire deposition. Data were collected by scanning the  $\Delta$  angle across the [311] reflection of cubic GaN. A series of  $\Delta$  scans were collected with 20 data points per scan. It took  $\approx 30$  sec to complete a full scan and begin the next. Because of the different lattice parameters for the two materials (0.452 nm for GaN and 0.435 nm for SiC), the two reflections are expected to be separated by  $1.5^\circ$  in  $\Delta$ . The diffracted intensity and the Ga  $K\alpha$  fluorescence intensity were recorded at a rate of 1 sec per data point. After the growth, standard *ex situ* characterization measurements were performed, including Rutherford backscattering spectrometry to determine the coverage and composition of the film and scanning electron microscopy (SEM) to assess the island shape and the degree of coalescence.

## III. RESULTS

### A. Real-time measurements

The x-ray diffraction data is presented in Fig. 2. Only the tail of the SiC peak is visible in the  $\Delta$  scan at the start of the growth. A small peak corresponding to GaN is visible after 500 sec, and by 1000 sec, the peak is well developed. Data for 1500, 2000, and 2500 sec are also shown. There are several notable features to this data. First, the peak position does not change and there is no significant shoulder or secondary peak at the high-angle side. Another interesting feature of the data is that the peak widths, which are extracted by fitting with a Lorentzian line shape and deconvolution

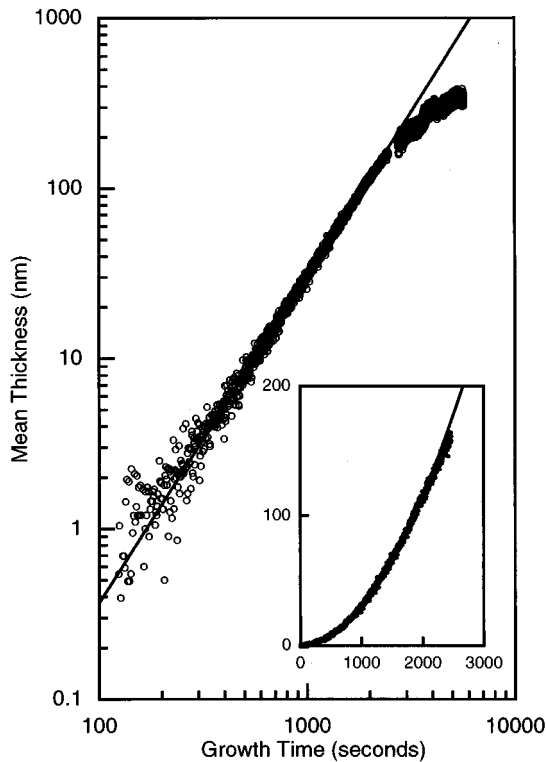


FIG. 3. Ga  $K\alpha$  intensity as a function of time during the film growth. The inset shows the early-time dependence on a linear scale with a  $t^{1.92}$  power-law curve as a guide to the eye.

with the resolution, are about  $0.5^\circ$  at all times. This suggests a domain size of around 6 nm. This distance coincides almost exactly with the mean spacing between misfit dislocations expected for the 3.8% lattice mismatch between the two materials. However, the high density of other defects, such as stacking faults, present in the GaN film makes such a simple interpretation of the data suspect. Note that the direction of the  $\Delta$  scan is such that it measures the domain size in the plane of the surface. Thus a  $\Delta$  scan is not directly sensitive to the vertical height of the islands. A third interesting feature of the data is that the integrated area under each scan does not increase linearly with growth time. This suggests either that there is a structural change taking place during the growth or that the growth rate is not linear. To directly address this question, we turn to the fluorescence measurement, which is a direct measure of the Ga surface coverage.

The gallium fluorescence data collected simultaneously with the diffraction data is shown in Fig. 3 from 100 sec after the start of the film growth to 5700 sec, when the growth was stopped. The gap in the data near 2700 sec was during the time that the collimator in front of the Si(Li) detector was replaced with a smaller collimator to reduce dead time. The data points after the gap are scaled to correct for the change in count rate. The data can be fit by a power law in time with an exponent of  $1.92 \pm 0.05$  before 2000 sec. The maximum growth rate, which occurred between 1000 and 2000 sec was 357 nm/h. This can be compared to the maximum possible growth rate of 800 nm/h, calculated from the Ga impingement rate and assuming that no Ga escapes back into the vapor. After 2000 sec, the growth rate falls away from the power-law behavior, becoming linear. The point of the breakaway from the power-law behavior coincides with the coalescence

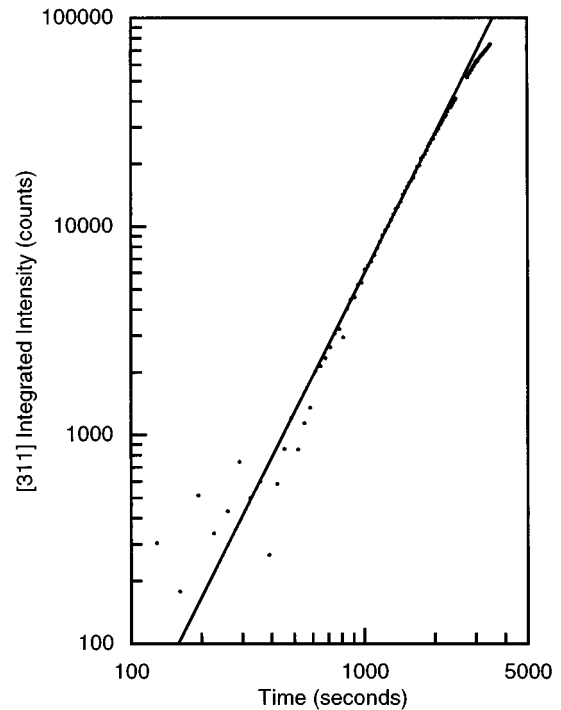


FIG. 4. Integrated intensity of the GaN [311] reflection from 100 sec after starting the film growth to 4000 sec.

of islands into a continuous film. This is known from examination of other film growths stopped just before the end of the power-law behavior. At late times, the system exhibits a constant growth rate of 199 nm/h.

A more complete analysis of the crystallinity of the growing film can be obtained from integrated intensities of the detector scans over the [311] GaN reflection. Integrated intensities of the entire data set (including those in Fig. 2) at 30-sec time intervals are shown in Fig. 4. The data follow nearly the same power-law behavior as the fluorescence data in Fig. 3. The early-time power-law persists until about 2000 sec, when the data begin to smoothly fall away until, it reaches linear growth at 3500 sec. The best-fit early-time exponent was  $2.22 \pm 0.05$ , which is slightly larger than the value derived from the Ga  $K\alpha$  data. Therefore, the diffraction data are in close agreement with the Ga fluorescence measurements. However, a slight improvement in crystalline perfection during the growth is suggested by the more rapid increase of the diffracted intensity.

## B. Post-growth measurements

Additional information about the crystallinity of the final film was obtained by *in situ* x-ray scans after the completion of the film growth. Figure 5 shows a two-dimensional intensity map as a function of  $\theta$  and  $\Delta$ . The map includes both the SiC [311] and the GaN [311] reflections. The largest peak is from the 5- $\mu\text{m}$  SiC substrate layer and has a width of  $0.4^\circ$  in the  $\theta$  direction. The smaller peak is from the 350-nm GaN film and has a width of  $1.35^\circ$  in the  $\theta$  direction. This width is comparable to the present state of the art for  $\beta$ -GaN (Refs. 12 and 14) and shows that our film growth method can pro-

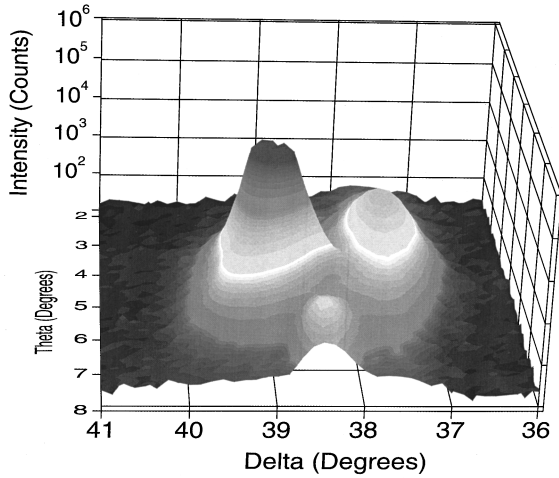


FIG. 5. Surface plot of the SiC and GaN [311] reflections after the completion of the film growth. The  $\Delta$  angle is relative to the horizontal plane, while the  $\theta$  angle has an arbitrary offset.

duce single-crystal material. A small additional peak is visible in the contour map near  $\theta=6^\circ$  and is attributed to defects in the GaN layer.

Figure 6 shows a scanning electron micrograph of the same GaN film discussed above. The image is consistent with our interpretation of the real-time x-ray data since it is apparent that island coalescence has already occurred. However, there are some pinholes in the film. The islands are elongated along either the  $[110]$  or  $[\bar{1}\bar{1}0]$  directions and the two possible orientations produce a large-scale pattern. Coalescence of islands appears to be more efficient along their long direction, leading to very long chains in some areas. Some islands also appear to have facets with roughly a  $(111)$  orientation.

#### IV. DISCUSSION

##### A. Growth kinetics

Since the fluorescence experiment measures the total number of Ga atoms illuminated, we use the cluster volume, in units of atoms per cluster, as a measure of its size. Ac-

ording to nuclear growth models,<sup>4,5</sup> the volume of a nucleus grows with a power-law dependence

$$V_{\text{clust}} \propto t^m. \quad (1)$$

The particular value of the exponent is determined by the growth mechanism. This dependence is only strictly valid for nuclei with a radius larger than  $(D\tau)^{1/2}$ , where  $D$  is the surface diffusion coefficient. For the two cases discussed above, direct deposition and capture growth,  $m$  has a value between 2 and 3. Sigsbee shows that small nuclei may have a slower time dependence.<sup>4</sup> For example, nuclei whose growth is dominated by capture exhibit  $m=1$  growth when their radii are smaller than  $(D\tau)^{1/2}$  and  $m=2$  at later times. In general, the island size distribution  $N(V_{\text{clust}}, t)$  must also be taken into account before a direct comparison with fluorescence coverage data can be made. This is because the experiment measures the Ga coverage  $\theta(t)$ , where

$$\theta(t) = N_{\text{tot}} \bar{V}, \quad (2)$$

$\bar{V}$  is the mean island size, and  $N_{\text{tot}}$  is the areal density of islands. The critical assumption in the dynamic scaling approach is that there should be only one characteristic size in the problem.<sup>16–21</sup> Then, the mean island size should have the same time dependence as an individual island. Electron microscopy measurements on samples with different GaN deposition times have found no significant change in  $N_{\text{tot}}$  after about 1000 sec. Therefore, the data are interpreted as being a measurement of the late-time evolution of noninteracting nuclei. In this regime, we may write  $\theta(t) \propto t^m$ . We have not studied the density of nuclei at earlier times.

The experimentally determined exponent of  $1.92 \pm 0.05$  is very close to  $m=2$ . The fact that the data can be fit with a single exponent over several orders of magnitude and that the exponent is very close to 2 leads us to believe that the data are indicative of two-dimensional island growth. The mechanism of growth is most likely capture at the edges of nuclei.

##### B. Island shape and behavior near coalescence

For  $m=2$ , the active sites for growth are around the edge of the growing islands. In theory, each island grows laterally, but its thickness does not increase beyond a certain value that is determined very early in the growth. In order to estimate the thickness of the islands, a second sample was prepared with only 1000 sec of film growth. *Ex situ* microscopic investigation of this sample with scanning electron microscopy, optical microscopy, and Rutherford backscattering spectrometry shows that the islands are  $\approx 33$  nm in thickness and about 300 nm in diameter. If we assume that the coalescence of nuclei coincides with the growth rate falling away from its early-time power law, then from Fig. 3, the island thickness is about 100 nm at coalescence; from Fig. 6, the lateral nuclear dimensions are on the order of  $1 \mu\text{m}$ . These observations suggest that the lateral growth velocity of nu-

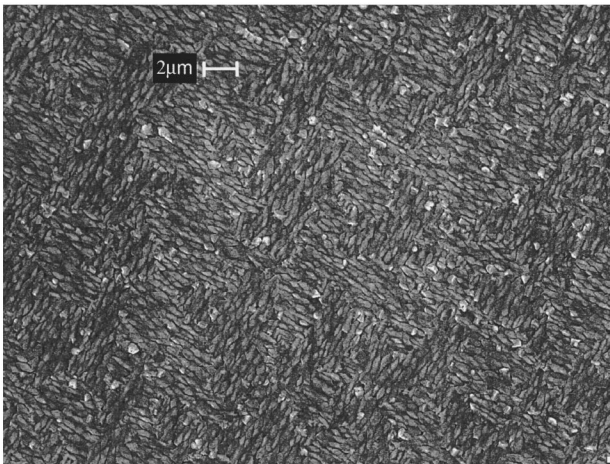


FIG. 6. Scanning electron micrograph of the film after growth.

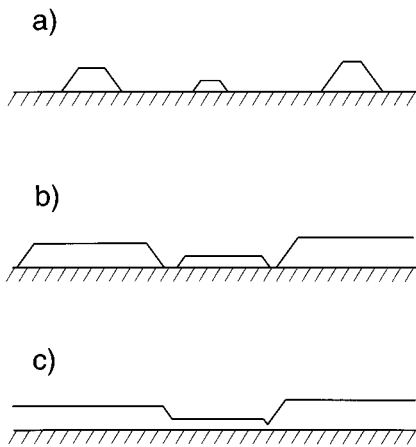


FIG. 7. Schematic diagram of the growth and coalescence of thin disk-shaped clusters.

clei is about ten times the vertical growth velocity. Island coalescence prevents additional lateral growth; however, vertical growth continues at a slower, constant rate after coalescence.

So far, we have ignored the microscopic nature of the active sites that lead to the quasi-two-dimensional growth. One possibility is that surface steps and kinks are the active sites. For nearly flat-topped islands as we have in our growths, steps are concentrated near the island edges. Then as islands coalesce the film becomes continuous and the number of steps decreases to a steady-state value. Similar effects are expected for growth at (111) facets at the edges of islands. The SEM result in Fig. 6 shows some evidence for this effect; the elongated island growth is similar to GaSb growth on GaAs(001) where the asymmetry is attributed to a difference in growth rate of Sb-terminated (111)<sub>B</sub> facets relative to Ga-terminated (111)<sub>A</sub> facets.<sup>15</sup> Figure 6 also shows evidence for facets on some islands. A model of growth at (111) facets is illustrated in Fig. 7. Figure 7(a) shows isolated islands that grow laterally towards each other. Figure 7(b) shows the beginning of coalescence and finally Fig. 7(c) shows complete coalescence. In this model, coalescence leads to a reduction in facet area and consequently the growth rate slows down.

### C. Influence of defects and strain

*Ex situ* x-ray-diffraction measurements on our samples suggest that the GaN films contain a high density of stacking faults. This is consistent with previous transmission electron microscopy studies of GaN growth on  $\beta$ -SiC.<sup>14</sup> The large defect density determines the domain size of the film, which is smaller than the lateral size of the islands but comparable to their height. We have investigated the possibility of an increasing domain size due to annealing. Both  $\theta$  scans, and  $\Delta$  scans have been performed during the growth (see Fig. 2, for example) and have not detected any change in the lateral domain size. Annealing at temperatures up to 800 °C did not produce any observable changes. However, stacking faults are known to be difficult to anneal out. A high density of stacking faults in fcc materials causes peak broadening and additional peaks in power-diffraction scans.<sup>22–24</sup> The small extra peak in Fig. 5 is believed to be from this effect. Our *ex situ* measurements also indicate that the films are highly strained. Therefore, the peak position in diffraction scans is determined by a combination of strain and stacking faults.

## V. CONCLUSIONS

In conclusion, we have used x-ray-scattering techniques to perform real-time studies of the nucleation kinetics of  $\beta$ -GaN on SiC(001) during GS MBE. The scaling of the data suggest that GaN islands initially grow in a quasi-two-dimensional mode. This leads to a reduction in growth rate once island coalescence is reached. The quasi-two-dimensional island growth mode is a very interesting phenomenon with important consequences for the fabrication of thin-film structures.

## ACKNOWLEDGMENTS

This work was supported by the National Science Foundation under Grants Nos. DMR-9311772 (Cornell High Energy Synchrotron Source), DMR-881858A02 (Cornell Materials Science Center), and ECS-9411668 (thin-film growth-x-ray-diffraction equipment grant).

\*Present address: Department of Chemical Engineering, University of Massachusetts at Amherst, Amherst, MA 01003.

<sup>1</sup>J. W. Matthews, *Epitaxial Growth* (Academic, New York, 1975).

<sup>2</sup>J. Y. Tsao, *Materials Fundamentals of Molecular Beam Epitaxy* (World Scientific, Singapore, 1993).

<sup>3</sup>F. Family and J. G. Amar, *Mater. Sci. Eng. B* **30**, 149 (1995).

<sup>4</sup>R. A. Sigsbee, *J. Appl. Phys.* **42**, 3904 (1971).

<sup>5</sup>A. V. Osipov, *Thin Solid Films* **227**, 111 (1993).

<sup>6</sup>D. Walton, *J. Chem. Phys.* **37**, 2182 (1962); D. Walton, T. N. Rhodin, and R. W. Rollins, *ibid.* **38**, 2698 (1963).

<sup>7</sup>J. A. Venables, G. D. Spiller, and M. Hanbucken, *Rep. Prog. Phys.* **47**, 399 (1984).

<sup>8</sup>D. P. Adams, L. L. Tedder, T. M. Mayer, B. S. Swartzentruber, and E. Chason, *Phys. Rev. Lett.*, **74**, 5088 (1995).

<sup>9</sup>R. F. Davis, Z. Sitar, B. E. Williams, H. S. Kong, H. J. Kim, J. W. Palmour, J. A. Edmond, J. Ryu, J. T. Glass, and C. H. Carter,

*Mater. Sci. Eng. B* **1**, 77 (1988).

<sup>10</sup>S. Strite and H. Morcoç, *J. Vac. Sci. Technol. B* **10**, 1237 (1992); S. Strite, M. E. Lin, and H. Morcoç, *Thin Solid Films* **231**, 197 (1993).

<sup>11</sup>The role of hydrogen passivation in limiting the surface reaction rate also appears to be important. C. R. Abernathy (private communication).

<sup>12</sup>R. C. Powell, N.-E. Lee, Y.-W. Kim, and J. E. Greene, *J. Appl. Phys.* **73**, 189 (1993).

<sup>13</sup>Certified Scientific Software, Cambridge, MA.

<sup>14</sup>M. J. Paisley, Z. Sitar, J. B. Posthill, and R. F. Davis, *J. Vac. Sci. Technol.* **7**, 701 (1988).

<sup>15</sup>J. M. Kang, M. Nouaoura, L. Lassabatre, and A. Rocher, *J. Cryst. Growth* **143**, 115 (1994).

<sup>16</sup>T. Vicsek and F. Family, *Phys. Rev. Lett.*, **52**, 1669 (1984).

<sup>17</sup>F. Family and P. Meakin, *Phys. Rev. Lett.* **61**, 428 (1988).

- <sup>18</sup>M. C. Bartelt and J. W. Evans, Phys. Rev. B **46**, 12 675 (1992); Surf. Sci. **298**, 421 (1993).
- <sup>19</sup>J. G. Amar, F. Family, and P. M. Lam, Phys. Rev. B **50**, 8781 (1994).
- <sup>20</sup>C. Ratsch, A. Zangwill, P. Smilauer, and D. D. Vvedensky, Phys. Rev. Lett. **72**, 3194 (1994).
- <sup>21</sup>J. G. Amar and F. Family, Phys. Rev. Lett. **74**, 2066 (1995).
- <sup>22</sup>B. E. Warren, J. Appl. Phys. **34**, 1973 (1963).
- <sup>23</sup>H. Holloway and M. S. Klamkin, J. Appl. Phys. **40**, 1681 (1969).
- <sup>24</sup>M. S. Paterson, J. Appl. Phys. **23**, 805 (1952).